

# Photomineralization in a boreal hydroelectric reservoir: a comparison with natural aquatic ecosystems

Nicolas Soumis · Marc Lucotte · Catherine Larose ·  
François Veillette · René Canuel

Received: 26 May 2006 / Accepted: 16 June 2007 / Published online: 13 September 2007  
© Springer Science+Business Media B.V. 2007

**Abstract** In order to evaluate the role of photochemistry in the carbon dioxide (CO<sub>2</sub>) generation from a 10-year-old boreal reservoir, the photomineralization of dissolved organic matter (DOM) was assessed and compared to a boreal river as well as to boreal and temperate lakes during July and August, 2003. Sterile water samples were irradiated by sunlight over the whole photoperiod and subsequently analyzed for CO<sub>2</sub>. Mean energy-normalized apparent photochemical yield of CO<sub>2</sub> (an index of DOM photoreactivity normalized for the energy absorbed by samples) was significantly higher in the reservoir ( $27.7 \pm 13.0 \text{ mg CO}_2 \cdot \text{m}^{-3} \cdot \text{kJ}^{-1}$ ) and the boreal river ( $35.8 \pm 2.3 \text{ mg CO}_2 \cdot \text{m}^{-3} \cdot \text{kJ}^{-1}$ ) than in the boreal lakes ( $15.5 \pm 5.1 \text{ mg CO}_2 \cdot \text{m}^{-3} \cdot \text{kJ}^{-1}$ ). The DOM photoreactivity of the temperate lakes ( $20.9 \pm 8.1 \text{ mg CO}_2 \cdot \text{m}^{-3} \cdot \text{kJ}^{-1}$ ) was not statistically different from any type of boreal water bodies. There was no significant difference in either the integrated photoproduction of CO<sub>2</sub> ( $273\text{--}433 \text{ mg CO}_2 \cdot \text{m}^{-2} \cdot \text{d}^{-1}$ ) or the potential photochemical contribution to CO<sub>2</sub> diffusive fluxes (56–92%) among these water bodies. DOM photoreactivity was significantly affected by the cumulative hydrological residence time (CHRT)

when considering the whole data set. However, when considering only the boreal water bodies, iron (Fe) and manganese (Mn) also intervened. The fact that DOM photoreactivity was related to CHRT as well as to Fe and Mn concentrations, which are respectively permanent and long-lasting features of the reservoir, suggests that the photoproduction of CO<sub>2</sub> is not likely to decrease over time. This process may therefore play a substantial role in the long-term CO<sub>2</sub> emissions from boreal reservoirs during the summer, its potential contribution to CO<sub>2</sub> diffusive fluxes being estimated at  $56 \pm 29 \%$ .

**Keywords** Photomineralization · Photoreactivity · Carbon dioxide · Dissolved organic matter · Boreal hydroelectric reservoir · Greenhouse gas production

## Introduction

The renewed interest in limnology for the photochemical transformations of dissolved organic matter (DOM) has led to a better understanding of the fate of carbon within aquatic ecosystems (e.g., Salonen and Vähätalo 1994; Granéli et al. 1996; Bertilsson and Tranvik 2000). Photochemical transformations of aquatic DOM are assumed to be ubiquitous (Bertilsson and Tranvik 2000) and generate several photoproducts among which carbon dioxide (CO<sub>2</sub>) is by far the most abundant (Miller and Moran 1997; Anesio et al. 1999; Bertilsson and Tranvik 2000).

N. Soumis (✉) · M. Lucotte · C. Larose ·  
F. Veillette · R. Canuel  
Institute of Environmental Sciences/GEOTOP,  
University of Québec at Montréal, Succ. Centre-Ville,  
C.P. 8888, Montreal, QC, Canada H3C 3P8  
e-mail: nicolas.soumis@internet.uqam.ca

Since DOM photomineralization may occur at rates similar to respiration (Granéli et al. 1996), this abiotic process can play a substantial role in the CO<sub>2</sub> emission budgets of freshwater ecosystems.

Although it is widely recognized that boreal reservoirs constitute anthropogenic sources of CO<sub>2</sub> for the atmosphere (Duchemin et al. 1995; Kelly et al. 1997; Huttunen et al. 2002, 2003), the role of photochemical reactions in this context has yet to be addressed. Degradation of flooded soils has been identified as the major source of CO<sub>2</sub> emissions from reservoirs during the first years of impoundment (Kelly et al. 1997). However, carbon content of flooded soils is limited and cannot account for the long-term CO<sub>2</sub> emissions from boreal reservoirs (Houel 2003). The latter likely stem, at least in part, from the degradation of organic matter inputs from the watershed (Duchemin et al. 1996; Weissenberger et al. 1999; Huttunen et al. 2003). Since sunlight is able to break down biologically recalcitrant terrigenous DOM into CO<sub>2</sub> (Bertilsson and Allard 1996; Vähätalo et al. 1999; Tranvik and Bertilsson 2001; Jonsson et al. 2001), photomineralization may play a substantial role in the long-term CO<sub>2</sub> emissions of reservoirs. Moreover, both the impoundment and operation phases may cause particular environmental conditions in reservoirs (Ford 1990; Thornton 1990; Straškraba 1998; Soumis et al. 2005). Consequently, the photochemical fate of DOM in these perturbed ecosystems may be different than in natural water bodies. For instance, it is likely that reservoirs' relatively short hydrological residence times optimize the supply of fresh, photodegradable terrigenous DOM in comparison to natural lakes. In addition, the frequent absence of thermal stratification in reservoirs due to important water outflows allows hypolimnetic DOM—which is normally hidden from sunlight in natural lakes during the summer—to be transferred into the photic zone where it can be photomineralized.

Herein, we report the results of a study addressing the photoproduction of CO<sub>2</sub> from a boreal reservoir. In this paper, “photoproduction” refers to CO<sub>2</sub> which is generated solely from DOM via both direct absorption of photon energy (Zepp and Cline 1977) and indirect photo-sensitization by reactive oxygen species formed through nitrate-mediated reactions (Brezonik and Fulkerson-Brekken 1998) as well as photo-Fenton reactions (Voelker et al. 1997) in

sterile water samples. We first determine and compare some photochemical aspects (DOM photo-reactivity, daily photoproduction of CO<sub>2</sub> and photochemical contribution to CO<sub>2</sub> diffusive fluxes) of the reservoir with natural lacustrine and riverine ecosystems. Since DOM characteristics, water pH, iron (Fe) and manganese (Mn) concentrations as well as hydrological residence time of water bodies are likely to affect photochemical processes (Sunda and Kieber 1994; Voelker et al. 1997; Reche et al. 1999; Grzybowski 2000; Lindell et al. 2000; Gennings et al. 2001; Anesio and Granéli 2003), we evaluate the influence of these variables on the photoreactivity of DOM. Finally, we discuss the implications of the photoproduction of CO<sub>2</sub> in the long-term emissions of boreal reservoirs.

## Material and methods

### Study zones

The study was conducted during July and August 2003 under boreal (James Bay) and temperate latitudes (Eastern Townships). Located on the Canadian Shield in the Lower Middle North of Québec, Canada (53–54° N; 72° W), James Bay is composed of igneous and metamorphic rocks. Black spruce (*Picea mariana*) open forests with thick lichen mats (*Cladina rangiferina*) and bogs are common in this taiga region. The Eastern Townships stretch over the southeastern part of Québec (45° N; 72° W). This area is characterized by a sedimentary geology and is covered by temperate mixed and broadleaf forests.

The boreal subset of water bodies comprises the 10-year-old Laforge-1 reservoir, a segment of the LaGrande River and three small lakes (Table 1). The Laforge-1 reservoir is part of the LaGrande hydroelectric complex and is located downstream of two reservoirs, Caniapiscou and Laforge-2. The temperate subset is composed of three lakes of small to large size. In order to account for reservoir's spatial heterogeneity, ten sampling sites distributed between its thalweg (open zone: 6 sites) and coves (protected zone: 4 sites) were selected. Lakes were sampled in their littoral and pelagic zones while the river's thalweg was sampled in a shallow and a deep area, for a total of two sites per water body.

**Table 1** Main characteristics of the sampled water bodies

Water body	Location (latitude; longitude)	Watershed area (km <sup>2</sup> )	Lake area (km <sup>2</sup> )	$z_{\text{mean}}$ (m)	CHRT <sup>a</sup> (d)	[P] <sub>tot</sub> ( $\mu\text{mol}\cdot\text{l}^{-1}$ )	[Chl-a] ( $\mu\text{mol}\cdot\text{l}^{-1}$ )
Laforge-1 reservoir	54°20' N; 72°15' W	8,771	1,288	5.7	95/933 <sup>b</sup>	23.87	2.19
LaGrande River	53°46' N; 72°53' W	97,600	ND	ND	14	ND	ND
Lake 12	54°08' N; 72°40' W	8.0	2.15	4.7	1,816	20.58	1.26
Lake 17	54°07' N; 72°44' W	1.6	0.25	1.6	ND	22.47	1.93
Lake 378	53°52' N; 72°40' W	17.5	1.53	3.6	ND	27.75	2.05
Lake Fraser	45°22' N; 72°10' W	60.2	1.62	8.6	1,321	16.92	2.73
Lake Lovering	45°10' N; 72°09' W	38.1	4.89	9.7	630	17.09	3.89
Lake Memphrémagog	45°05' N; 72°15' W	1,764	102	15.5	620	ND	ND

<sup>a</sup> Cumulated hydrological residence time. For headwater lakes, CHRT is equivalent to hydrological residence time ( $\tau$ ). Otherwise, CHRT corresponds to the sum of  $\tau$  for upstream and considered water bodies

<sup>b</sup> Values for the coves and the thalweg of the reservoir, respectively

ND: Not determined

### Light and temperature profiles

Downwelling spectral irradiance ( $E_{d\lambda}$ ) for UV-B (305, 313, 320 nm), UV-A (340, 380, 395 nm) and photosynthetically active radiation (PAR; 400–700 nm) were measured on each site with a *Biospherical Instruments PUV-2500/2510* radiometer. Temperature profiles were recorded concomitantly with a built-in thermal probe. Spectral attenuation coefficients ( $K_{d\lambda}$ ) were determined from the slope of linear regressions of  $\ln E_{d\lambda}$  versus depth. Depth of spectral photic zones ( $z_{1\% \lambda}$ ) were then determined according to Eq. 1, where  $E_{d\lambda}(z_{1\% \lambda})$  is equivalent to 1% of the surface spectral irradiance ( $E_{d\lambda}(0)$ ):

$$z_{1\% \lambda} = \frac{\ln E_{d\lambda}(0) - \ln E_{d\lambda}(z_{1\% \lambda})}{K_{d\lambda}} \quad (1)$$

### CO<sub>2</sub> diffusive fluxes at the air/water interface

On each sampling site, 30-ml water samples were taken 15 cm below the air/water interface with 60-ml syringes for dissolved CO<sub>2</sub> analyses. Atmospheric CO<sub>2</sub> concentration was also measured. CO<sub>2</sub> diffusive fluxes ( $f\text{CO}_2$ ) were then calculated according to Fick's first law:

$$f\text{CO}_2 = k_{\text{CO}_2} \times ([\text{CO}_2]_{\text{surf}} - (p\text{CO}_{2\text{atm}} \times K_{\text{H}})) \quad (2)$$

where  $[\text{CO}_2]_{\text{surf}}$  is the actual CO<sub>2</sub> concentration at the surface of water and  $(p\text{CO}_{2\text{atm}} \times K_{\text{H}})$  the CO<sub>2</sub>

concentration that water would have if it were in equilibrium with the atmosphere.  $p\text{CO}_{2\text{atm}}$  is the atmospheric CO<sub>2</sub> partial pressure and  $K_{\text{H}}$  is the Henry's constant corrected for water temperature. The piston velocity constant for CO<sub>2</sub> ( $k_{\text{CO}_2}$ ) was calculated as follows:

$$K_{\text{CO}_2} = k_{600} \times \left( \frac{600}{\text{Sc}_{\text{CO}_2}} \right)^{0.67} \quad (3)$$

where  $k_{600}$ , the piston velocity normalized to a Schmidt number of 600, was estimated from wind speed measured at a height of 10 m ( $U_{10}$ ), according to Cole and Caraco (1998):

$$k_{600} = 2.07 + (0.215 \times U_{10}^{1.7}) \quad (4)$$

$\text{Sc}_{\text{CO}_2}$ , which represents the Schmidt number for carbon dioxide in Eq. 3, is calculated according to Eq. 5 (Wanninkhof, 1992), where  $T^{\circ}_{\text{w}}$  is the water surface temperature:

$$\text{Sc}_{\text{CO}_2} = 1911.1 - (118.11 \times T^{\circ}_{\text{w}}) + (3.4527 \times T^{\circ}_{\text{w}}^2) - (0.04132 \times T^{\circ}_{\text{w}}^3) \quad (5)$$

The empirical relationship from Cole and Caraco (1998) shown in Eq. 4 has a regression coefficient ( $r^2$ ) of 0.61, which induces a substantial variance in the estimation of  $k_{600}$  from wind speed measurements. These authors suspect that penetrative convection and rainfall may be responsible for the variance in  $k_{600}$  at a given wind speed. Although the variance in  $k_{600}$

estimates increases the uncertainty of CO<sub>2</sub> evasion rates, this was not accounted for in the diffusive flux data presented hereafter. According to an experiment conducted on a small oligotrophic temperate lake (Soumis 2006), we established that CO<sub>2</sub> diffusive flux measurements using Eq. 4 represented 80–130% of CO<sub>2</sub> losses as calculated by the mass budget. Considering the good agreement between both approaches, we assume the CO<sub>2</sub> diffusive flux measurements to be acceptable.

### Sampling and irradiation of water samples

A peristaltic pump fitted with a nylon filter (1.2 µm pore size) and a graduated tube was used to collect a 10-l integrated sample of the photic zone ( $z_{1\%PAR}$ ). Following its collection, the pH of the integrated water sample was measured. Filtered aliquots (0.45 µm) were also taken for the determination of spectral absorbances, DOM color and carbon content, as well as dissolved Fe and Mn concentrations. Mercuric dichloride (HgCl<sub>2</sub>) at 0.01 N and nitric acid (HNO<sub>3</sub>) at 2.0 N were used as preservatives for DOM and Fe/Mn samples, respectively.

Upon return to the field laboratory, the integrated water sample was sterilized by filtration (polyether-sulfone filters, 0.2 µm pore size). Sterile water was then transferred into transparent and dark irradiation cells (three of each), which consisted of 20-cm long tubes with an internal radius of 2 cm. Transmittance of the transparent quartz cells (TS cells) was 88–94% between 305 nm and 700 nm. Dark borosilicate control cells (DS cells) were covered with opaque heat-shrinkable plastic. Both ends of the irradiation cells were sealed with paraffin film (*Parafilm*) and plugged with perforated rubber stoppers. Cells were then placed transversally onto rectangular plastic frames, which held TS and DS cells in triplicate.

Frames were placed at a depth of 0.01 m in a lake near the laboratory (irradiation site). The depth positioning of the frames was ensured by buoys, which allowed the frames to follow wave movements, thereby maintaining a water layer of constant thickness above the cells. Samples were irradiated during 24 h (as to include full day-night cycle) over which the surface spectral irradiance ( $E_{d\lambda}(0)$ ) was monitored every 10 min. In order to assess the optical climate of the boreal and temperate irradiation sites,

several irradiance profiles were performed during the course of the campaign. Following irradiation, 30-ml aliquots of water were withdrawn from the cells with 60-ml syringes for CO<sub>2</sub> analyses. In order to prevent CO<sub>2</sub> loss, cell sampling was performed with cannulas that were inserted through perforated stoppers. Aliquots were also taken for the determination of spectral absorbances.

### Chemical analyses

CO<sub>2</sub> analyses were carried out within a few hours following the sampling of irradiation cells. A *Varian Star 3400* gas chromatograph (GC) was equipped with a 1-ml sampling loop, a steel packed *Hayesep-Q* column (200-mm long, 3 mm in diameter, 80/100 mesh) in an isothermal oven at 50°C, and a thermal conductivity detector (TCD). Helium (30 ml·min<sup>-1</sup>) was used as the carrier gas. Water samples in syringes were first allowed to reach ambient temperature before being equilibrated with 30 ml of ultrapure nitrogen (N<sub>2</sub>) according to the headspace technique described by McAuliffe (1971). Water was then gently discarded and the gaseous phase was injected into the GC. CO<sub>2</sub> concentrations in water were calculated according to the solubility coefficient corrected for temperature (Wilhelm et al. 1977).

Carbon content of DOM samples (DOC) was determined with a *Shimadzu TOC-5000A* analyzer, using the platinum-catalyzed high-temperature combustion method. Total dissolved Fe and Mn concentrations of the integrated sample were measured using a *GBC-906AA* atomic absorption apparatus with a graphite furnace. Since Fe (Voelker et al. 1997; Gao and Zepp 1998) and Mn (Sunda and Kieber 1994) can both act as catalysts for photochemical reactions involving DOM in aquatic ecosystems, their concentrations in terms of molarity were summed for subsequent data analyses.

### Spectral absorption coefficients and DOM color index

Measurements of spectral absorbance ( $A_{\lambda}$ ) at 305, 313, 320, 340, 380, 395 and 400–700 nm (every 50 nm) were performed with a *Beijing Purkinje*

General Instrument TU-1800S UV–VIS split beam spectrophotometer. Since the absorbance of water samples declines with the photodegradation of DOM (Reche et al. 1999; Lindell et al. 2000), we considered the spectral absorbances of the integrated water sample as the initial spectral absorbances and the mean of the post-irradiated TS cell spectral absorbance values as the final spectral absorbances. Mean spectral absorbances ( $A_{\lambda}\mu$ ) for irradiated samples were calculated according to initial and final spectral absorbance values.  $A_{\lambda}\mu$  were then used to determine the spectral absorption coefficients ( $a_{\lambda}$ ) of the irradiated samples according to Eq. 6, where  $l$  (0.10 m) is the pathlength of the spectrophotometric quartz cell:

$$a_{\lambda} = \frac{2.303 \times A_{\lambda}\mu}{l} \quad (6)$$

The absorption coefficient of the integrated water sample was also calculated at 440 nm ( $a_{440}$ ) according to Eq. 6. We then computed the  $a_{440}$ :[DOC] ratio which constitutes an index of DOM color (Reche et al. 1999). Since humic matter is more chromophoric than autochthonous compounds (Meili 1992), the  $a_{440}$ :[DOC] ratio is expected to increase as the proportion of terrigenous organic matter input augments within a water body.

#### DOM photoreactivity

Energy-normalized apparent photochemical yield ( $APY_{CO_2}$ ) is the potential of a given volume of water to generate  $CO_2$  per unit of light energy absorbed and therefore constitutes an index of DOM photoreactivity. This parameter must not be confused with apparent quantum yield ( $\phi$ ) which is the dimensionless ratio of the number of photoproduct molecules generated per quantum of a given wavelength absorbed (Leifer 1988; Miller et al. 2002). Since  $APY_{CO_2}$  is computed on an energy basis, this index allows for a direct comparison of water samples irradiated under different sunlight conditions. Action spectra were not established; it was therefore impossible to determine which wavelengths were actually involved in DOM photomineralization. Consequently, we assumed that photons comprised between 305 nm and 700 nm were all effective in generating  $CO_2$  (Granéli et al. 1998; Vähätalo et al. 2000), which justifies the use of the term “apparent” photochemical yield in this study.

In order to compute  $APY_{CO_2}$ , we first calculated  $E_{d\lambda}(z)$  for the irradiation site. PAR irradiance data from the radiometer are expressed in  $\mu\text{einstein}\cdot\text{m}^{-2}\cdot\text{s}^{-1}$ . Therefore, to estimate the power density of PAR in  $\text{W}\cdot\text{m}^{-2}$ ,  $E_{dPAR}(0)$  was normalized for 550 nm. Since variations in photon flux density ( $\pm 2.02 \mu\text{mol quanta}\cdot\text{m}^{-2}\cdot\text{s}^{-1}$ ) and energy ( $\pm 130 \text{ kJ}\cdot\text{mol quanta}^{-1}$ ) are relatively low between 400 nm and 700 nm (Leifer 1988), we consider the estimation from the mid-value of 550 nm to be valid. Second, conversion into spectral exposure ( $E_{\lambda}$ ) for each irradiation depth was performed by integrating  $E_{d\lambda}(z)$  versus time. According to the specifications in Miller (1998),  $E_{\lambda}$  was then used to compute the spectral energy absorbed by TS cells ( $E_{a\lambda}$ ), knowing their  $a_{\lambda}$  (Eq. 6), optical pathlength ( $L = 0.0354 \text{ m}$ ) and lateral surface area ( $S = 0.0226 \text{ m}^2$ ):

$$E_{a\lambda} = [E_{\lambda} - (E_{\lambda} \times e^{-a_{\lambda} \times L})] \times S \quad (7)$$

Third, the dose of UV energy absorbed by TS cells ( $E_{aUV}$ ) at a given irradiation depth was determined by integrating discrete  $E_{a\lambda}$  data from 305 nm to 395 nm versus  $\lambda$ . The sum of  $E_{aUV}$  and  $E_{aPAR}$  was considered to reflect the total energy absorbed by TS cells ( $E_t$ ) at the irradiation site during the irradiation period. We then calculated the difference in mean  $CO_2$  concentrations between TS and DS cells ( $\Delta[CO_2] = \text{TS} - \text{DS}$ ), which represents the net photoproduction of  $CO_2$  (Granéli et al. 1996).  $APY_{CO_2}$  was finally computed according to Eq. 8:

$$APY_{CO_2} = \frac{\Delta[CO_2]}{E_t} \quad (8)$$

#### Photoproduction of $CO_2$ and contribution to $CO_2$ diffusive fluxes

During the 24-h irradiation periods, surface spectral irradiance (305–700 nm) was registered under different sky conditions: sunny, partly cloudy and cloudy/rainy. Irradiance data were sorted with respect to the latitude where they were collected (boreal/temperate) and the mean of each data set was used to calculate a specific daily exposure (SDE) for the three particular sky conditions in each study zone. A daily exposure value assumed to be representative of a typical mid-summer day (TSE) for each study zone was then



computed by averaging the three SDE values of the corresponding latitude.

Daily integrated photoproduction of CO<sub>2</sub> (DIP<sub>CO<sub>2</sub></sub>) indicates the rate at which CO<sub>2</sub> is photoproduced during a typical mid-summer day. Since DIP<sub>CO<sub>2</sub></sub> is eventually limited by the total depth of the water column, sampling sites shallower than  $z_{1\%PAR}$  were rejected from mean DIP<sub>CO<sub>2</sub></sub> calculations. In order to compute DIP<sub>CO<sub>2</sub></sub>, we first determined the amount of light energy absorbed by water samples at four depth intervals evenly distributed along the photic zone using  $K_{d\lambda}$  and  $a_{\lambda}$  from each sampling site as well as the corresponding TSE value. We then multiplied these energy values by APY<sub>CO<sub>2</sub></sub> to calculate a CO<sub>2</sub> photoproduction rate for each depth. DIP<sub>CO<sub>2</sub></sub> was finally obtained by integrating these discrete photoproduction rates as a function of depth.

Photochemical contribution to CO<sub>2</sub> diffusive fluxes (PCF<sub>CO<sub>2</sub></sub>) is the ratio of DIP<sub>CO<sub>2</sub></sub> to  $fCO_2$  under the particular environmental conditions encountered during sampling. In this case however, DIP<sub>CO<sub>2</sub></sub> was computed using the SDE corresponding to the sky conditions encountered during sampling rather than TSE. Since PCF<sub>CO<sub>2</sub></sub> is influenced by parameters which may fluctuate substantially during the day (light regime, wind conditions and, to a lesser extent, CO<sub>2</sub> concentration in water), this ratio provides an instantaneous comparison rather than a time-integrated index of both phenomena.

## Results

### Physicochemical and optical parameters

Physicochemical parameters of the sampled water bodies appear in Table 2. Mean DOC concentrations ranged from 3.38 to 5.38 mg C·l<sup>-1</sup>. The reservoir's mean DOC content was higher than that of the boreal river, but lower than those of the boreal and temperate lakes. According to the  $a_{440}$ :[DOC] ratios, DOM from the reservoir was the least colored, thereby indicating lower concentrations of allochthonous DOM than for the other types of water bodies. The boreal water bodies were circumneutral (pH 6.48 to 6.56), while the temperate lakes were slightly basic, with a mean pH value of 7.92. Mean Fe and Mn concentrations among the sampled water bodies ranged from 0.51 to 1.42 μmol·l<sup>-1</sup> and from 0.04 to 0.11 μmol·l<sup>-1</sup>,

respectively. The highest concentrations of these metals were observed in the reservoir and the boreal lakes. Overall, the sampled water bodies were very similar in their optical features. Mean spectral photic zone ( $z_{1\%I}$ ) for UV-B (305–320 nm), UV-A (340–395 nm) and PAR varied between 0.34–0.52 m, 0.51–1.54 m and 6.49–7.83 m, respectively.

In order to highlight the spatial heterogeneity within the reservoir, its thalweg and coves were considered separately in Table 2. Although DOM color (Mann–Whitney *U* test;  $P = 0.0700$ ), DOC concentrations (Student *t* test;  $df = 8$ ;  $P = 0.1104$ ) and Mn concentrations (Kruskal–Wallis test;  $P = 0.3374$ ) were statistically comparable between the thalweg and coves of the reservoir, significant differences were found in their pH conditions (Student's *t* test;  $df = 8$ ;  $P = 0.0411$ ) and Fe concentrations (Student *t* test;  $df = 8$ ;  $P = 0.0030$ ).

### Photochemical parameters

Cumulative exposure during irradiation of water samples varied between 4.4 and 12.4 kJ·m<sup>-2</sup> (305–700 nm). Corresponding energy absorbed by TS cells ranged from 3.6 to 16.2 kJ. Photochemical parameters of the sampled water bodies are shown in Table 3. Mean APY<sub>CO<sub>2</sub></sub> for the sampled water bodies ranged from 15.5 to 35.8 mg CO<sub>2</sub>·m<sup>-3</sup>·kJ<sup>-1</sup>. No relation was found between APY<sub>CO<sub>2</sub></sub> and either cumulative exposure ( $r^2 = 0.14$ ;  $P = 0.0688$ ;  $n = 24$ ) or energy absorbed by TS cells ( $r^2 = 0.03$ ;  $P = 0.4426$ ;  $n = 24$ ). This suggests that our approach, which consisted in irradiating samples on different days (distinct light regimes), did not significantly affect results. Mean APY<sub>CO<sub>2</sub></sub> for the river and the reservoir (whole) were significantly higher than those of the boreal lakes (ANOVA test on ln-transformed data;  $P = 0.0225$ ; followed by a Tukey–Kramer HSD test on ln-transformed data). The temperate lakes were statistically similar to all types of boreal water bodies. In the reservoir, mean APY<sub>CO<sub>2</sub></sub> for the coves was significantly higher than that for the thalweg (Welsh ANOVA *F* test;  $P = 0.0463$ ).

Mean DIP<sub>CO<sub>2</sub></sub> ranged from 273 to 433 mg CO<sub>2</sub>·m<sup>-2</sup>·d<sup>-1</sup> and no difference was found among the distinct types of water bodies (ANOVA test;  $P = 0.4816$ ). Likewise, there was no difference between the coves and the thalweg of the reservoir

**Table 2** Mean physicochemical parameters of the integrated water sample (photic zone) of the sampled water bodies

Water body	[DOC] (mg C·l <sup>-1</sup> )	<i>a</i> <sub>440</sub> : [DOC] (l·m <sup>-1</sup> · mg C <sup>-1</sup> )	pH (pH units)	[Fe] (μmol· l <sup>-1</sup> )	[Mn] (μmol· l <sup>-1</sup> )
Boreal lakes	4.73 ± 1.13	0.500 ± 0.296	6.56 ± 0.10	1.42 ± 0.26	0.11 ± 0.07
Temperate lakes	5.38 ± 1.66	0.470 ± 0.121	7.92 ± 0.12	0.51 ± 0.20	0.04 ± 0.01
Boreal river	3.38 ± 0.31	0.572 ± 0.019	6.48 ± 0.01	0.66 ± 0.01	0.10 ± 0.03
Boreal reservoir (whole)	4.12 ± 0.76	0.374 ± 0.177	6.53 ± 0.09	1.63 ± 0.38	0.11 ± 0.03
Boreal reservoir (coves)	3.64 ± 0.44	0.272 ± 0.051	6.46 ± 0.06	1.99 ± 0.29	0.12 ± 0.04
Boreal reservoir (thalweg)	4.44 ± 0.79	0.442 ± 0.202	6.58 ± 0.08	1.38 ± 0.17	0.10 ± 0.02

Indicated errors are standard deviations. [DOC] = dissolved organic carbon concentration; *a*<sub>440</sub>: [DOC] = DOM color index; [Fe] = iron concentration; [Mn] = manganese concentration

**Table 3** Mean photochemical parameters and CO<sub>2</sub> diffusive fluxes of the sampled water bodies

Water body	APY <sub>CO<sub>2</sub></sub> (mg CO <sub>2</sub> ·m <sup>-3</sup> · kJ <sup>-1</sup> )	DIP <sub>CO<sub>2</sub></sub> <sup>a</sup> (mg CO <sub>2</sub> · m <sup>-2</sup> ·d <sup>-1</sup> )	(CO <sub>2</sub> <sup>b</sup> (mg CO <sub>2</sub> · m <sup>-2</sup> ·d <sup>-1</sup> ))	PCF <sub>CO<sub>2</sub></sub> <sup>a</sup> (% of <i>f</i> CO <sub>2</sub> )
Boreal lakes	15.5 ± 5.1	274 ± 63	+333 ± 224	92 ± 22
Temperate lakes	20.9 ± 8.1	273 ± 63	+691 ± 1,385	ND
Boreal river	35.8 ± 2.3	433 ± 89	+802 ± 157	71 ± 11
Boreal reservoir (whole)	27.7 ± 13.0	332 ± 154	+779 ± 282	56 ± 29
Boreal reservoir (coves)	39.9 ± 12.7	376 ± 63	+632 ± 139	73 ± 27
Boreal reservoir (thalweg)	19.6 ± 3.1	297 ± 56	+877 ± 321	45 ± 26

Indicated errors are standard deviations. APY<sub>CO<sub>2</sub></sub> = Energy-normalized apparent photochemical yield; DIP<sub>CO<sub>2</sub></sub> = daily integrated photoproduction of CO<sub>2</sub>; (CO<sub>2</sub> = CO<sub>2</sub> diffusive fluxes at the air/water interface; PCF<sub>CO<sub>2</sub></sub> = photochemical contribution to CO<sub>2</sub> diffusive fluxes

<sup>a</sup> Sampling sites where the total depth was shallower than the calculated photic zone were rejected from calculations

<sup>b</sup> A positive sign indicates a CO<sub>2</sub> efflux (source); a negative sign indicates a CO<sub>2</sub> influx (sink)

ND: Not determined

(Student *t* test; *df* = 7; *P* = 0.4808). At the moment of sampling (±3 h around noon), boreal water bodies were all sources of CO<sub>2</sub>, with mean fluxes ranging from +333 to +802 mg CO<sub>2</sub>·m<sup>-2</sup>·d<sup>-1</sup>. The mean diffusive flux for temperate lakes was +691 mg CO<sub>2</sub>·m<sup>-2</sup>·d<sup>-1</sup>. Temperate lakes were generally sources of CO<sub>2</sub>, with the exception of Lake Lovering, which acted as a sink for atmospheric CO<sub>2</sub> (−204 ± 82 mg CO<sub>2</sub>·m<sup>-2</sup>·d<sup>-1</sup>). This situation explains the high variability of the mean flux figure for these lakes (Table 3). Finally, PCF<sub>CO<sub>2</sub></sub> of the boreal water bodies were statistically comparable (ANOVA test; *P* = 0.5981), varying from 56 to 92%.

#### Environmental factors affecting DOM photoreactivity

Several factors can affect the rate of photochemical reactions in aquatic ecosystems. DOM color or origin

(Tranvik and Bertilsson 2001; Reitner et al. 2002) and hydrological residence time (Grzybowski 2000; Lindell et al. 2000; Waiser and Robarts 2000) can impact the composition and reactivity of DOM. Other factors such as pH (Gennings et al. 2001; Molot et al. 2005), Fe (Voelker et al. 1997; Gao and Zepp 1998) and Mn (Sunda and Kieber 1994) contents also influence photochemical reactions as they affect physicochemical conditions or intermediary reactions which promote DOM photomineralization. The scatter plots of Fig. 1 explore individually the eventual relations between the DOM photoreactivity index (APY<sub>CO<sub>2</sub></sub>) and six environmental factors. Results show that, with the exception of the cumulated hydrological residence time (CHRT; Fig. 1A), all the other environmental parameters tested here show no relation (Fig. 1C–F), absence of normality for the residuals (Shapiro–Wilk test result < 0.05; Fig. 1B, D, and E) and/or an odd distribution of data, which weakened analysis (Fig. 1E).

In aquatic ecosystems, complex interactions, such as competition or covariation, can occur between several environmental factors affecting DOM photoreactivity (Reche et al. 1999), thereby complicating the issue of explicative analyses. Therefore, in order to decipher the environmental variables which most contributed to the variations observed in DOM photoreactivity ( $APY_{CO_2}$ ), we performed stepwise multiple regression analyses. Step order was mixed, probability to enter was 0.15 and probability to leave was 0.01. Independent variables considered were the same as in Fig. 1 and when necessary, data were  $\ln$ -transformed in order to obtain linearity and a normal distribution of residuals. Two models were constructed; one including the whole data set (A) and the other comprising only the boreal water bodies (B). Model A indicates that CHRT ( $P < 0.0001$ ) was the only variable that explained the variability in  $APY_{CO_2}$  indexes ( $r^2 = 0.58$ ;  $P < 0.0001$ ;  $n = 20$ ; RMSE = 0.2684). As for the boreal water bodies, model B indicates that both CHRT ( $P < 0.0001$ ) and  $\Sigma_{[Fe, Mn]}$  ( $P = 0.0019$ ) influenced  $APY_{CO_2}$  indexes. Neither of the other environmental variables tested here had a significant effect on DOM photoreactivity and were rejected from both models.

## Discussion and conclusions

### Comparison of the water bodies under study

Based on measurements performed over a wide range of physicochemical conditions in different climatic regions, it has been shown that photoproduction rates of DIC in natural lakes are remarkably comparable (Granéli et al. 1998; Bertilsson and Tranvik 2000). Our study corroborates this finding as we observed no statistical difference in the daily integrated photoproduction of  $CO_2$  ( $DIP_{CO_2}$ ) among the different types of boreal and temperate water bodies studied (Table 3). Moreover, the mean  $DIP_{CO_2}$  values from this study (273–433  $mg\ CO_2 \cdot m^{-2} \cdot d^{-1}$ , which correspond to 74–118  $mg\ C \cdot m^{-2} \cdot d^{-1}$ ) are fairly similar to photoproduction rates of dissolved inorganic carbon (DIC) from Swedish lakes (44–171  $mg\ C \cdot m^{-2} \cdot d^{-1}$ ) with DOC concentrations ranging from 3.9 to 19.4  $mg\ C \cdot l^{-1}$  (Granéli et al. 1996). In addition, the photochemical contribution to  $CO_2$  diffusive fluxes ( $PCF_{CO_2}$ ) did not vary significantly among boreal water bodies.

Despite these similarities in both  $DIP_{CO_2}$  and  $PCF_{CO_2}$  from the sampled water bodies, significant differences were observed in their DOM photoreactivity.  $APY_{CO_2}$  indexes indicate that the DOM from both the reservoir and the river was significantly more photoreactive than that of the boreal lakes. Dissimilarities in DOM photoreactivity were also observed between the coves and the thalweg of the reservoir, a situation that did not occur between the littoral and pelagic zones of the natural lakes. Furthermore, when the reservoir was divided into distinct hydrological zones, there was a striking similarity in DOM photoreactivity indexes between the thalweg and the lakes on the one hand, and the coves and the river on the other (Table 3).

### Influence of cumulated hydrological residence time, Fe and Mn on DOM photoreactivity

Photo-Fenton reactions, which involve Fe, are known to promote the photo-oxidation of DOM through the formation of hydroxyl radicals ( $HO^\bullet$ ) in aquatic ecosystems (Voelker et al. 1997). However, it has been demonstrated that this process is optimal in acidic waters and that its importance rapidly decrease as pH increases. Between pH values of 4 and 7, the relative contribution of mechanisms involving  $HO^\bullet$  to DOM photo-oxidation declines from 42 to 25% and becomes negligible when pH is around 9 (Molot et al. 2005). Since the boreal water bodies under study were slightly acidic (6.48–6.56), it is likely that photo-Fenton reactions were involved in the photo-mineralization of DOM, the relative contribution of these mechanisms being estimated at ca. 30%. In temperate lakes however, higher pH conditions (7.78–8.12) likely reduced the impact of photo-Fenton reactions. The influence of pH conditions on photo-Fenton reactions might thus constitute an explanation as to why  $\Sigma_{[Fe, Mn]}$  was rejected from model A, but entered in model B.

According to water level fluctuation observations for Laforge-1, water outflows occurred during the sampling of the reservoir, causing a slight, but gradual reduction in its pool level. During drawdowns, which are common in hydroelectric reservoirs, water masses trapped in coves move toward the thalweg (Ford 1990). When this occurs in Laforge-1, most of the water flowing through the thalweg comes from



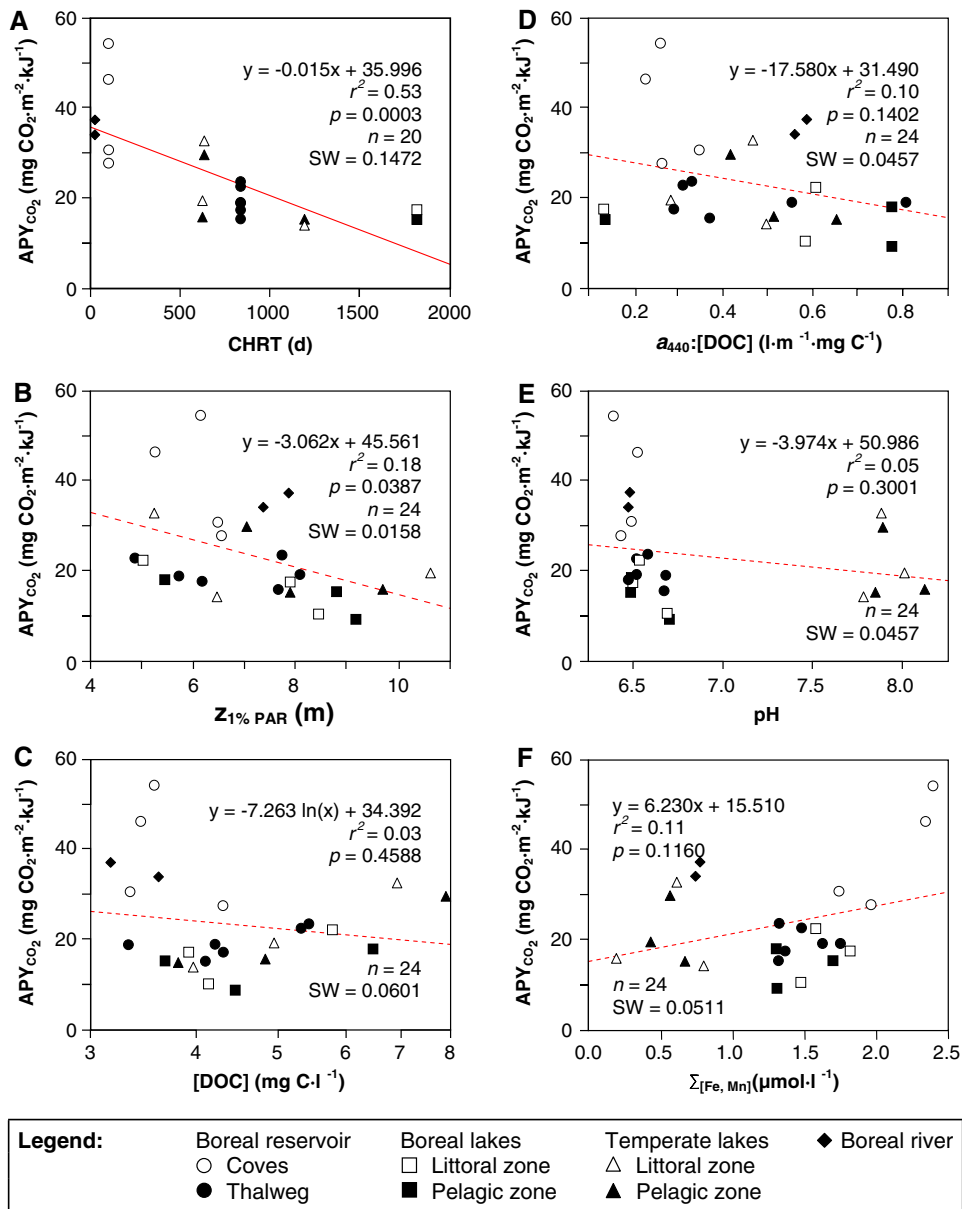


**Fig. 1** Scatter plots attempting to correlate the energy-normalized apparent photochemical yield ( $APY_{CO_2}$ ) with environmental factors. Statistics of the best possible fit and Shapiro–Wilk test results (SW) are indicated for each plot. (A) Cumulated hydrological residence time (CHRT). (B) Depth of

the photic zone for PAR ( $z_{1\%PAR}$ ). (C) DOC concentration ([DOC]). (D) DOM color index ( $a_{440}:[DOC]$ ). (E) pH conditions (pH). (F) Summed concentrations of iron and manganese ( $\Sigma_{[Fe, Mn]}$ )

upstream reservoirs (Caniapiscau and Laforge-2). Consequently, DOM from the thalweg is about an order of magnitude older (CHRT for the thalweg is the sum of hydrological residence times for Caniapiscau, Laforge-2 and Laforge-1: 933 days) than DOM reaching the coves through runoff from the watershed

(CHRT for the coves is assumed to be equivalent to the hydrological residence time for Laforge-1: 95 days). In addition, there was a significant difference in  $\Sigma_{[Fe, Mn]}$  between the thalweg ( $1.48 \mu\text{mol}\cdot\text{l}^{-1}$ ) and the coves ( $2.11 \mu\text{mol}\cdot\text{l}^{-1}$ ) of Laforge-1 (ANOVA test;  $P = 0.0035$ ). The marked contrast in both CHRT

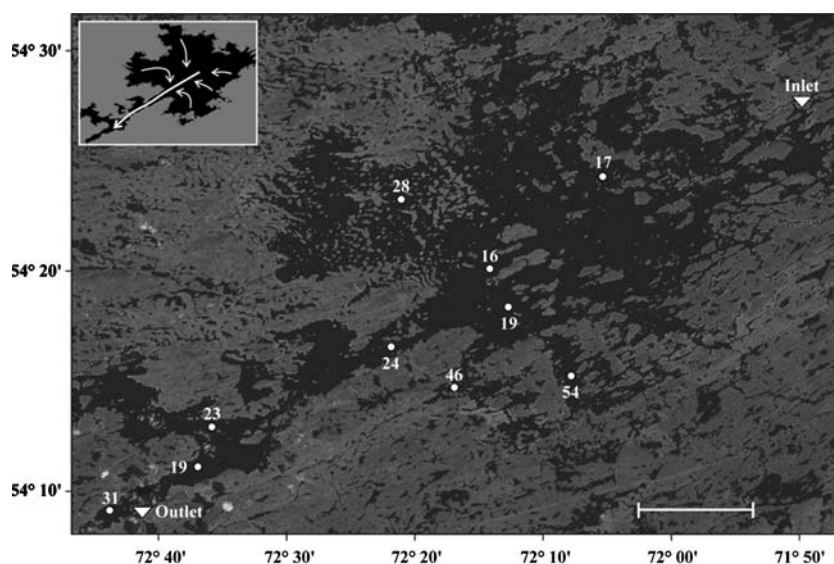
and  $\Sigma_{[\text{Fe}, \text{Mn}]}$  parameters between the thalweg and the coves appeared to generate a particular spatial distribution of DOM photoreactivity in Laforge-1. Superimposing  $\text{APY}_{\text{CO}_2}$  data on a map of Laforge-1 in Fig. 2 suggests the absence of a longitudinal gradient (i.e., along the main axis of the reservoir) in the  $\text{APY}_{\text{CO}_2}$  indexes. From the inlet to the outlet of the reservoir, DOM photoreactivity was not prone to variation and remained relatively low. However, there was a transversal gradient in DOM photoreactivity, with  $\text{APY}_{\text{CO}_2}$  values increasing toward the coves. Such a spatially contrasted response in DOM photoreactivity was not observed in any of the natural water bodies sampled.

#### Implications for the carbon cycle and $\text{CO}_2$ diffusive fluxes

This study supports the fact that DOM photomineralization is a significant mechanism in the carbon dynamics of aquatic ecosystems, at least during the summer. Based on calculations from mean daily integrated photoproduction rates of  $\text{CO}_2$  ( $\text{DIP}_{\text{CO}_2}$ ), this study indicates that between 0.13% and 0.49% of the DOM pool within the photic zone of the water bodies under study was photomineralized into  $\text{CO}_2$  on a daily basis during the sampling period (July–August 2003). Calculated mean daily decrease in DOM was

very similar for the reservoir ( $0.26 \pm 0.10\%$ ), boreal and temperate lakes ( $0.20 \pm 0.5\%$  and  $0.15 \pm 0.02\%$ , respectively), but higher for the boreal river ( $0.49 \pm 0.09\%$ ). In addition, a comparison with metabolic processes (Ahrens and Peters 1991; D. Planas, pers. comm.) indicates that mean  $\text{DIP}_{\text{CO}_2}$  corresponded to ca. 37, 40, and 15% of summer epilimnetic planktonic respiration of the reservoir, boreal and temperate lakes, respectively. These values are slightly higher than the results from Granéli et al. (1996), who determined that summer photoproduction of DIC in Swedish lakes is equivalent to 7–25% of the planktonic community respiration. DOM photomineralization therefore appears to be an important term within the summer carbon budget of aquatic ecosystems, especially in the case of boreal water bodies, as assessed during this study. In addition, as reported by some previous studies (Salonen and Vähätalo 1994; Granéli et al. 1996; Lindell et al. 2000), photomineralization appears to be a process that significantly contributes to  $\text{CO}_2$  supersaturation in these waters. One must however keep in mind that the contribution of photomineralization to the carbon budget of water bodies depends on the relative importance of the photic zone, which is influenced by both the total depth and DOM quantity or color. In relatively shallow aquatic ecosystems with low DOM contents where the photic zone represents an important fraction of the whole water column such as those assessed in

**Fig. 2** Spatial distribution of DOM photoreactivity within the Laforge-1 reservoir. Indicated values are  $\text{APY}_{\text{CO}_2}$  (in  $\text{mg CO}_2 \cdot \text{m}^{-3} \cdot \text{kJ}^{-1}$ ). The insert (upper left corner) shows the suspected circulation of water masses within the reservoir during the sampling period



this study, photomineralization will have a stronger impact on the carbon cycle than in deeper, more colored ones (Jonsson et al. 2001).

With regard to GHG emissions, DOM photomineralization has important implications for boreal reservoirs. Following the transient trophic upsurge which leads to a drastic boost in GHG production after the impoundment phase, anthropogenic CO<sub>2</sub> emissions from reservoirs decrease over the years (St-Louis et al. 2000; Duchemin et al. 2002). This decrease is attributable to the slow decline of microbial activity within flooded soils and the water column, as carbon and nutrients in flooded soils are gradually exhausted (Kelly et al. 1997). Despite the noticeable impact of this phenomenon on the GHG budget of reservoirs, some may still possess high rates of GHG emissions several decades after their impoundment (St-Louis et al. 2000; Duchemin et al. 2002). A fraction of long-term CO<sub>2</sub> emissions likely stems from the mineralization (including photomineralization) of allochthonous DOM, as proposed by literature (Duchemin et al. 1996; Weissenberger et al. 1999; Huttunen et al. 2003). The fact that DOM photoreactivity in boreal water bodies is affected by the cumulated hydrological residence time as well as Fe and Mn concentrations indicates that DOM photomineralization is mainly influenced by features which are not likely to vary to a great extent over time within boreal reservoirs. Consequently, we conclude that in boreal reservoirs older than Laforge-1 (i.e., >10-year-old) with similar environmental conditions, high DOM photoreactivity during the summer is also likely to be observed. DOM photomineralization may therefore play a significant role in long-term CO<sub>2</sub> emissions from boreal reservoirs, its potential contribution representing slightly more than half of CO<sub>2</sub> diffusive fluxes measured at the air/water interface. Although this situation is likely to occur during most of the open water season, the temporal limitation of the present study does not allow for extrapolation beyond the summer.

**Acknowledgements** The authors thank Lewis Molot (York University), Yves Prairie (UQAM), Peter Dillon (Trent University) and Sebastian Sobek (Uppsala Universitet) for their precious advice on the experimental protocol, as well as Serge Paquet, Sophie Tran and Élisabeth Turcotte from UQAM for their assistance on the field and in the laboratory. Two anonymous reviewers provided helpful comments on the

manuscript. This study was funded by the Canadian Department of Fisheries and Oceans (DFO) as well as the Natural Sciences and Engineering Research Council of Canada (NSERC) through a scholarship to the first author and a strategic project grant (#STP 224191-99).

## References

- Ahrens MA, Peters RH (1991) Plankton community respiration: relationships with size distribution and lake trophy. *Hydrobiologia* 224(1):77–87
- Anesio AM, Granéli W (2003) Increased photoreactivity of DOC by acidification: Implications for the carbon cycle in humic lakes. *Limnol Oceanogr* 48(2):735–744
- Anesio AM, Tranvik LJ, Granéli W (1999) Production of inorganic carbon from aquatic macrophytes by solar radiation. *Ecology* 80(6):1852–1859
- Bertilsson S, Allard B (1996) Sequential photochemical and microbial degradation of refractory dissolved organic matter in a humic freshwater system. *Arch Hydrobiol Beih Ergebn Limnol* 48:133–141
- Bertilsson S, Tranvik LJ (2000) Photochemical transformation of dissolved organic matter in lakes. *Limnol Oceanogr* 45(4):753–762
- Brezonik PL, Fulkerson-Brekken J (1998) Nitrate-induced photolysis in natural waters: Controls on concentrations of hydroxyl radical photo-intermediates by natural scavenging agents. *Environ Sci Technol* 32(19):3004–3010
- Cole JJ, Caraco NF (1998) Atmospheric exchange of carbon dioxide in low-wind oligotrophic lake measured by the addition of SF<sub>6</sub>. *Limnol Oceanogr* 43(4):647–656
- Duchemin É, Lucotte M and Canuel R (1996) Source of organic matter responsible for greenhouse gas emissions from hydroelectric complexes of the boreal regions. In: Bottrell SH (ed) *Proceedings of the Fourth International Symposium on the Geochemistry of the Earth's Surface*, Ilkley (UK), July 1996. University of Leeds Press, Leeds, pp 393–396
- Duchemin É, Lucotte M, Canuel R, Chamberland A (1995) Production of the greenhouse gases CH<sub>4</sub> and CO<sub>2</sub> by hydroelectric reservoirs of the boreal region. *Global Biogeochem Cycles* 9(4):529–540
- Duchemin É, Lucotte M, St-Louis V, Canuel R (2002) Hydroelectric reservoirs as an anthropogenic source of greenhouse gases. *World Res Rev* 14(3):334–353
- Ford DE (1990) Reservoir transport processes. In: Thornton KW, Kimmel BL, Payne FE (eds) *Reservoir limnology: ecological perspectives*. John Wiley & Sons, Inc., New York, pp 15–41
- Gao H, Zepp RG (1998) Factors influencing photoreactions of dissolved organic matter in a coastal river of the southeastern United States. *Environ Sci Technol* 32(19):2940–2946
- Gennings C, Molot LA, Dillon PJ (2001) Enhanced photochemical loss of organic carbon in acidic waters. *Biogeochemistry* 52(3):339–354
- Granéli W, Lindell M, Tranvik L (1996) Photo-oxidative production of dissolved inorganic carbon in lakes of different humic content. *Limnol Oceanogr* 41(4):698–706

- Granéli W, Lindell MJ, de Faria BM, Estevez F (1998) Photoproduction of dissolved inorganic carbon in temperate and tropical lakes—dependence of wavelength band and dissolved organic carbon concentration. *Biogeochemistry* 43(2):175–195
- Grzybowski W (2000) Effect of short-term sunlight irradiation on absorbance spectra of chromophoric organic matter dissolved in coastal and riverine water. *Chemosphere* 40(12):1313–1318
- Houel S (2003) Dynamique de la matière organique terrigène dans les réservoirs boréaux. Ph. D. thesis, University of Québec at Montréal
- Huttunen JT, Alm J, Liikanen A, Juutinen S, Larmola T, Hammar T, Silvola J, Martikainen PJ (2003) Fluxes of methane, carbon dioxide and nitrous oxide in boreal lakes and potential anthropogenic effects on the aquatic greenhouse gas emissions. *Chemosphere* 52(3):609–621
- Huttunen JT, Väisänen TS, Hellsten SK, Heikkinen M, Nykänen H, Jungner H, Niskanen A, Virtanen MO, Lindqvist OV, Nenonen OS and Martikainen PJ (2002) Fluxes of CH<sub>4</sub>, CO<sub>2</sub>, and N<sub>2</sub>O in hydroelectric reservoirs Lokka and Porttipahta in the northern boreal zone in Finland. *Global Biogeochem Cycles* 16(1), doi: 10.1029/2000GB001316
- Jonsson A, Meili M, Bergström AK, Jansson M (2001) Whole-lake mineralization of allochthonous and autochthonous organic carbon in a large humic lake (Örträsket, N. Sweden). *Limnol Oceanogr* 46(7):1691–1700
- Kelly CA, Rudd JWM, Bodaly RA, Roulet NP, St-Louis VL, Heyes A, Moore TR, Schiff S, Aravena R, Scott KJ, Dyck B, Harris R, Warner B, Edwards G (1997) Increases in fluxes of greenhouse gases and methyl mercury following flooding of an experimental reservoir. *Environ Sci Technol* 31(5):1334–1344
- Leifer A (1988) The kinetics of environmental aquatic photochemistry. Theory and practice. American Chemical Society, Washington, DC
- Lindell MJ, Granéli HW, Bertilsson S (2000) Seasonal photoreactivity of dissolved organic matter from lakes with contrasting humic content. *Can J Fish Aquat Sci* 57(5):875–885
- McAuliffe C (1971) GC determination of solutes by multiple phase equilibration. *Chem Technol* 1(1):46–51
- Meili M (1992) Sources, concentrations and characteristics of organic matter in softwater lakes and streams of the Swedish forest region. *Hydrobiologia* 229:23–41
- Miller WL, Moran MA (1997) Interaction of photochemical and microbial processes in the degradation of refractory dissolved organic matter from a coastal marine environment. *Limnol Oceanogr* 42(6):1317–1324
- Miller WL, Moran MA, Sheldon WM, Zepp RG, Opsahl S (2002) Determination of apparent quantum yield spectra for the formation of biologically labile photoproducts. *Limnol Oceanogr* 47(2):343–352
- Miller WL (1998) Effects of UV radiation on aquatic humus: photochemical principles and experimental considerations. In: Hessen DO, Tranvik L (eds) *Aquatic humic substances: ecology and biogeochemistry*. Springer, New York, pp 125–141
- Molot LA, Hudson JJ, Dillon PJ, Miller SA (2005) Effect of pH on photo-oxidation of dissolved organic carbon by hydroxyl radicals in a coloured, softwater stream. *Aquat Sci* 67(2):189–195
- Reche IM, Pace L, Cole JJ (1999) Relationship of trophic and chemical conditions to photobleaching of dissolved organic matter in lake ecosystems. *Biogeochemistry* 44(3):259–280
- Reitner B, Herzig A, Herndl GJ (2002) Photoreactivity and bacterioplankton availability of aliphatic versus aromatic amino acids and protein. *Aquat Microb Ecol* 26(3):305–311
- Salonen K, Vähätalo A (1994) Photochemical mineralisation of dissolved organic matter in Lake Skjervatjern. *Environ Int* 20:307–312
- Soumis N (2006) Émissions de gaz à effet de serre à partir des réservoirs hydroélectriques: Aspects méthodologiques et évaluation des processus photochimiques. Ph. D. thesis, University of Québec at Montréal
- Soumis N, Lucotte M, Duchemin É, Canuel R, Weissenberger S, Houel S, Larose C (2005) Hydroelectric reservoirs as anthropogenic sources of greenhouse gases. In: Lehr JH, Keeley J (eds) *Water encyclopedia, vol 3: surface and agricultural water*. John Wiley & Sons, pp 203–210
- St-Louis VL, Kelly CA, Duchemin É, Rudd JWM, Rosenberg DM (2000) Reservoir surfaces as sources of greenhouse gases to the atmosphere: a global estimate. *BioSciences* 50(9):766–775
- Straškraba M (1998) Limnological differences between deep valley reservoirs and deep lakes. In: Straškrabová V, Vrba J (eds) *International review of hydrobiology. Proceeding of the Third International Conference on Reservoir Limnology and Water Quality, České Budejovice (Czech Republic), August 1997*, pp 1–12
- Sunda WG, Kieber DJ (1994) Oxidation of humic substances by manganese oxides yields low-molecular weight organic substrates. *Nature* 367:62–64
- Thornton KW (1990) Perspective on reservoir limnology. In: Thornton KW, Kimmel BL, Payne FE (eds) *Reservoir limnology: ecological perspectives*. John Wiley & Sons, Inc., New York, pp 1–13
- Tranvik LJ, Bertilsson S (2001) Contrasting effects of solar UV radiation on dissolved organic sources for bacterial growth. *Ecol Lett* 4(5):458–463
- Vähätalo AV, Salkinoja-Salonen M, Taalas P, Salonen K (2000) Spectrum of the quantum yield for photochemical mineralization of dissolved organic carbon in a humic lake. *Limnol Oceanogr* 45(3):664–676
- Vähätalo AV, Salonen K, Salkinoja-Salonen M, Hatakka A (1999) Photochemical mineralization of synthetic lignin in lake water indicates enhanced turnover of aromatic organic matter under solar radiation. *Biodegradation* 10(6):415–420
- Voelker BM, Morel FMM, Sulzberger B (1997) Iron redox cycling in surface waters: effects of humic substance and light. *Environ Sci Technol* 31(4):1004–1011
- Waiser MJ, Robarts RD (2000) Changes in composition and reactivity of allochthonous DOM in prairie saline lake. *Limnol Oceanogr* 45(4):763–774
- Wanninkhof R (1992) Relationship between gas exchange and wind speed over the ocean. *J Geophys Res - Atmosph* 97:7373–7382

- Weissenberger S, Duchemin É, Houel S, Canuel R and Lucotte M (1999) Greenhouse gas emissions and carbon cycle in boreal reservoirs. In: Rosa LP, dos Santos MA (eds) *Proceeding of the International Conference on Greenhouse Gas Emissions from Dams and Lakes*, Rio de Janeiro, December 1998. COPPE, Rio de Janeiro, pp 33–40
- Wilhelm E, Battino R, Wilcock R (1977) Low pressure solubility of gases in liquid water. *Chem Rev* 77(2):219–245
- Zepp RG, Cline DM (1977) Rates of direct photolysis in aquatic environments. *Environ Sci Technol* 11:359–366